Micromorphological Studies of Lithium Electrodes in Alkyl Carbonate Solutions Using in Situ Atomic Force Microscopy

Yaron S. Cohen, Yair Cohen, and Doron Aurbach*

Department of Chemistry, Bar-Ilan University, Ramat-Gan 52900, Israel

Received: July 18, 2000

The morphology of lithium electrodes in a variety of alkyl carbonate solutions was studied using in situ atomic force microscopy (AFM). We made use of a workstation specially built for the study of highly reactive electrochemical systems by AFM and other scanning probe techniques, based on an evacuable, vibration-protected glovebox. The electrolyte solution used was composed of propylene carbonate (PC), mixtures of ethylene carbonate (EC), dimethyl carbonate (DMC), diethyl carbonate (DEC), and Li salts from the following list: $LiPF_6$, $LiClO_4$, $LiAsF_6$, $LiN(SO_2CF_3)_2$, $LiN(SO_2CF_2CF_3)_2$, and $LiC(SO_2CF_3)_3$. We studied the effect of solution composition, prolonged storage, Li deposition, and dissolution at low and high current densities. The AFM imaging of these systems shows the complicated morphology of the Li electrodes that depend on the solution composition. We were able to clearly follow the nonuniform nature of Li deposition and dissolution in these systems. We were also able to follow by in situ AFM imaging critical events such as the onset of dendrite formation and the breakdown and repair of the surface films on lithium during Li dissolution at high current densities. The basic morphology of Li electrodes in alkyl carbonate solutions and the condition for the reversible behavior of Li electrodes is discussed.

Introduction

During the past three decades there have been intensive efforts to develop rechargeable batteries based on lithium metal anodes and liquid electrolyte solutions. The use of liquid electrolyte solutions in such batteries is important for maintaining their low internal resistance at a wide range of temperatures, and hence, for their operation at low temperatures.[1] However, over the years it has become clear that the combination of Li metal and any kind of liquid electrolyte solution is very problematic regarding rechargeable batteries, because of the high reactivity of the active metal with any relevant polar aprotic solvent or salt anion suitable for the composition of electrolyte solutions for Li batteries. A complicated surface chemistry is developed on Li electrodes in any polar aprotic solution. Initially, lithium metal is always covered by native surface films composed of lithium oxide (inner part), lithium hydroxide, and Li carbonate (outer part).[2] When lithium metal is introduced into any polar aprotic solution, a variety of reactions take place, including nucleophilic reactions between Li_2O, LiOH, and electrophilic solvents such as organic esters, alkyl carbonates, etc., to form organic Li salts,[3] and partial dissolution of pristine surface species and their replacement by insoluble products of the reactions of solution species on the reactive Li surface. Consequently, the active metal becomes covered by highly complex surface films with a mosaic-type structure on the microscopic level. The unavoidable presence of trace water in solutions further complicates the structure of the surface films that cover Li electrodes. Water hydrates many components comprising the surface films that cover the active metal, such as LiOH, Li_2O, and organic Li salts.[4] Thus, water, which hydrates the surface films, diffuses through them and reacts with lithium within the films to form LiOH (with hydrogen gas as the coproduct), and even possibly LiH.[4] Most of the organic and inorganic Li salts precipitate as thin films on lithium and conduct Li ions. Hence, the surface films that cover Li electrodes in any polar aprotic solution behave like a solid electrolyte interphase, which is an electronic insulator (thus providing the active metal with corrosion protection), but allow ion transport through it under an electrical field.[6] Li deposition in most of the commonly used electrolyte solutions that are usually composed of Li salts in polar aprotic solvents (e.g., ethers, esters, alkyl carbonates, and their combinations) is very dendritic.[7−10] Most of the failure mechanisms of rechargeable Li batteries with Li metal anodes are connected with Li dendrite formation in the batteries.[11] Dendrites form internal shorts between the anode and the cathode in the cells, and they are highly reactive with solution species and with air. Hence, their formation means fewer lithium and solution components. Exposure of dendritic Li to air causes a fire.

In spite of the above problems with the use of Li metal anodes in rechargeable batteries, there is an ongoing interest in R&D of Li metal-based secondary batteries due to the high energy density expected for these batteries.[12−14] Hence, basic morphological studies of lithium electrodes under different conditions may be an important prerequisite for their use in practical rechargeable batteries. Indeed, over the years, intensive work has been devoted to the morphological studies of Li electrodes.[7−9] Up until five years ago, the principal practical tool for studying Li morphology was scanning electron microscopy (SEM). This technique, which has to be used ex situ, has a major disadvantage of limited resolution. Since the lithium is always covered by electronically insulating surface films, as explained above, the electron beam of the SEM charges the surface electrically, and therefore it is usually impossible to obtain submicronic resolution of Li surfaces by SEM analysis. The appearance of atomic force microscopy (AFM) as an in situ tool for the study of electrochemical systems opened the door for in situ morphological studies of Li electrodes at very high resolution. We developed a special workstation for the analysis of highly

10.1021/jp002526b CCC: $19.00
Published on Web 12/05/2000

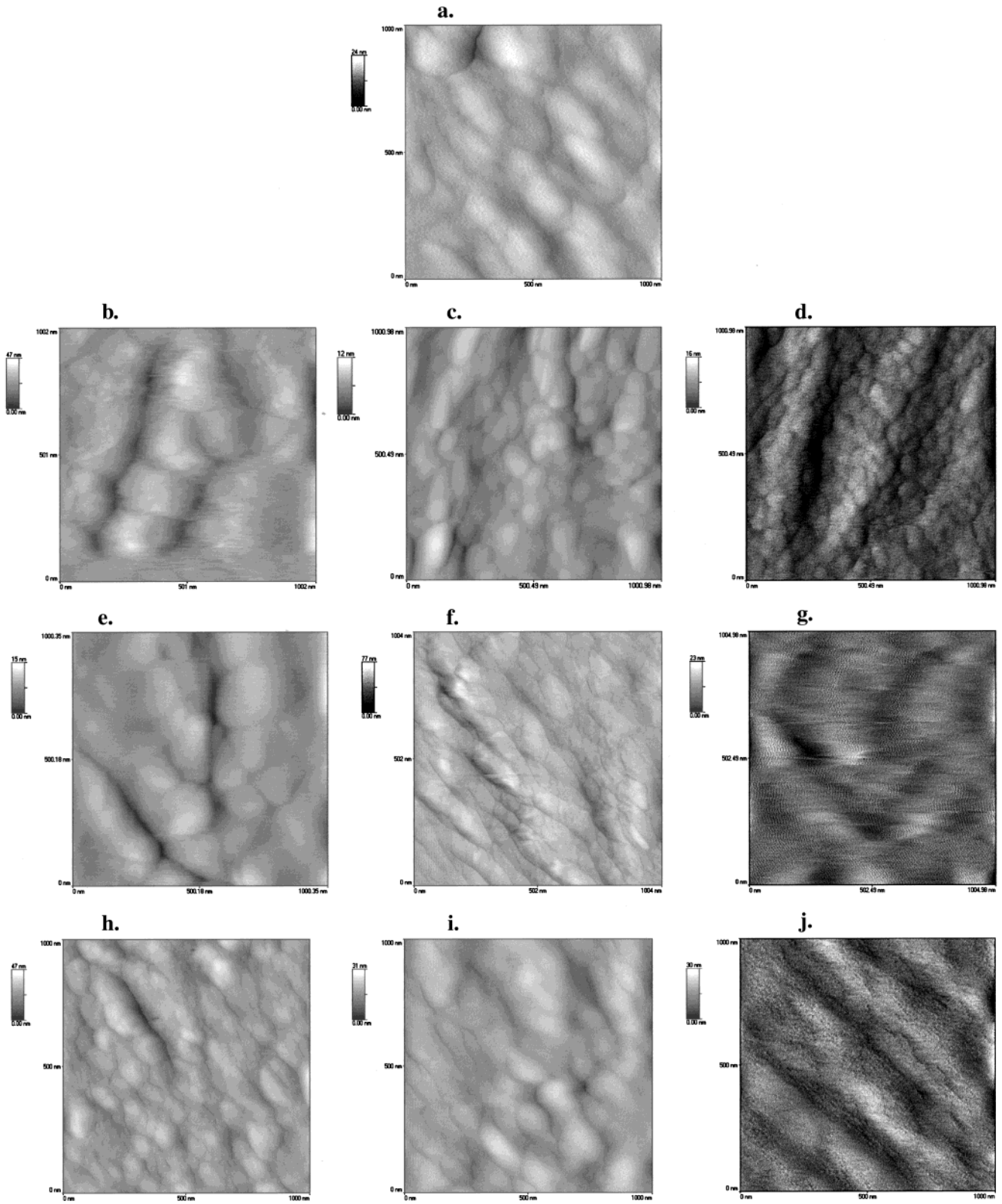

Figure 1. AFM images (1 × 1 μm) obtained at open circuit potential after 30 min storage in different solutions: (a) a typical reference AFM image of a Li electrode in argon before a solution is introduced; (b) $LiAsF_6$ (0.5 M)/EC-DMC 1:1; (c) $LiPF_6$ (0.5 M)/EC-DMC 1:1; (d) $LiPF_6$ (0.5 M)/PC; (e) $LiAsF_6$ (0.5 M)/PC; (f) $LiAsF_6$ (0.5 M)/EC-DEC 1:1; (g) $LiC(SO_2CF_3)_3$ (0.5 M)/EC-DEC 1:1; (h) $LiN(SO_2CF_3)_2$ (0.5 M)/EC-DEC 1:1; (i) $LiN(SO_2CF_2CF_3)_2$ (0.5 M)/EC-DEC 1:1; (j) $LiClO_4$ (0.5 M)/EC-DEC 1:1.

reactive electrochemical systems by atomic force and scanning tunneling microscopies (AFM, STM).[15] In several previous publications we demonstrated the gain in resolution and the high reliability of in situ micromorphological studies of Li electrodes by AFM.[16−18] The present work marks a further step in these studies. It involves intensive micromorphological studies of lithium electrodes in alkyl carbonate solutions of various Li salts, aimed at understanding major factors that determine the evolution of the observed morphology of lithium electrodes. The parameters explored included the solution composition,

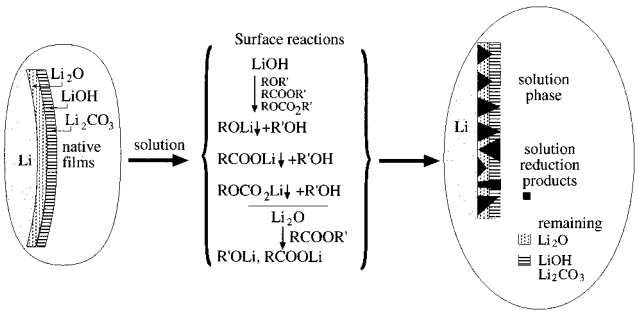

Figure 2. An illustration of the surface films on lithium as the active metal covered by a pristine surface layer (composed of Li_2O, Li_2CO_3, LiOH) is exposed to a nonaqueous electrolyte solution.

storage time, current densities, and the pristine surface morphology of the Li electrodes.

Experimental Section

Highly pure solvents (propylene carbonate, ethylene carbonate, dimethyl carbonate) were obtained from either Merck KGaA (Selectipure Series) or Tomiyama Inc. (Li battery grade), and could be used as received. Highly pure $LiAsF_6$ was obtained from FMC Inc. $LiN(SO_2CF_3)_2$ and $LiN(SO_2CF_2CF_3)_2$ were obtained from 3M Inc. $LiPF_6$ was obtained from Hashimoto Inc., and $LiC(SO_2CF_3)_3$ was received from Covalent Ass., USA. The special workstation that we built for the study of Li electrodes by AFM has already been described.[15] In brief, the Topometrix Discoverer model TMX 2010 series AFM system, as well as silicon nitride V-shaped tips with a constant force of 0.032 N/m from the same company, were used. The system was placed in a special evacuable, vibration-protected, homemade glovebox.[15] All the experiments were performed under a highly pure argon atmosphere, as already described.[15−18] It should be emphasized that it was proven that Li morphology could be very reliably studied by AFM in contact mode, although lithium is a soft metal. This can be explained by the fact that the AFM measurements probe the surface films that cover the active metal and are composed of Li salts, which are much harder than the lithium metal. Thus, they are not affected by the contact of the tip.

Results

1. Morphology of Li Electrodes in Open Circuit Solutions. Figure 1 shows a typical AFM image of a Li electrode under argon, and representative images of lithium electrodes in nine different solutions, as indicated. It is very significant that these images reflect pronounced submicronic differences between the pristine electrode morphology (Ar) and that of electrodes under solution. The images in Figure 1 also clearly show that the Li electrodes develop unique morphology in each solution. There are pronounced morphological differences among all the various electrodes in the different solutions under open circuit conditions. Hence, it appears that the different solution compositions induce variations in the Li morphology as well. These results seem to correlate with the scenario predicted for Li electrodes immersed in solution, as illustrated in Figure 2. Lithium electrodes are always introduced into the solutions while covered by native films, due to the unavoidable reaction of the active metal with trace O_2, CO_2, and H_2O in the glovebox atmosphere during preparation. Complicated reactions are expected between these pristine surface films, which are composed of nucleophilic species such as Li_2O and LiOH, and the electrophilic alkyl carbonates.

The evolution of further morphological changes upon storage depends on the reactivity of the solvent, and, even more importantly, on the solubility of the major reaction products between lithium and the solution components. This is clearly demonstrated in Figure 3. In EC-DEC solutions, pronounced changes are observed on a submicronic scale in the morphology of Li electrodes during storage under open circuit conditions (images 3a−c), while in a PC solution, the Li morphology is steady upon storage (3d−e). This is well understood in light of previous work in which the surface chemistry of lithium electrodes in various alkyl carbonate solutions was studied.[19] DEC is reduced on Li surfaces to CH_3CH_2OLi and $CH_3CH_2OCO_2Li$, and both are soluble in DEC.[19] The EC reduction product $(CH_2OCO_2Li)_2$[20] is insoluble in DEC solutions. Hence, we can attribute the morphological changes of Li in EC-DEC solutions upon storage to a dynamic surface chemistry, in which soluble species, which are the DEC reduction products, are initially present in the surface films. These are formed by instantaneous reactions of the electrode's active surface with all the solution components as it is exposed to the solution. However, upon storage, the soluble products are depleted from the surface films, while the content of insoluble surface species, such as the above-mentioned EC reduction product, which contains two carbonate groups, increases.

In PC (images 3d−e), the major surface species formed due to reaction between this solvent and lithium is the dicarbonate $CH_3CH(OCO_2Li)CH_2(OCO_2Li)$, which is insoluble in PC. Hence, from the very beginning of Li immersion in this solvent, there is no possibility of dissolution−deposition cycles, as in the case of the DEC solution described above. Hence, the major message from the studies described in this section is that a different composition of electrolyte solutions in terms of solvents, the salt used, and the presence of contaminants such as water, dictate unique Li electrode morphologies, probably due to unique surface reactions (which depend on the solution composition). Further morphological changes upon storage depend on the stability of the surface films formed initially (e.g., the solubility of surface species in the electrolyte solutions).

2. Dynamics of Li Deposition−Dissolution Cycles: General Description. It is possible to divide the lithium surfaces explored in the present study into three different categories:

1. Pronounced Li dendrites formed during Li deposition, which are of a micrometer scale and above.

2. Surface changes in the nanometer to submicrometer scale, which can be regarded as nucleation phenomena, the onset of dendrite formation, and/or important local reaction centers.

3. The rest of the Li surface area from the above features, in which only minor morphological changes can be probed during Li deposition and dissolution. These parts of the Li surfaces contract as the electrochemical processes of the Li electrodes become more prolonged and intensive.

It is well-known that Li deposition in most of the relevant electrolyte solutions ever mentioned in connection with lithium batteries is dendritic. It should be noted that AFM is not the appropriate tool for probing pronounced dendrite formation, due to the limitations in the tip's dimension and in the usual vertical scanning range of the instrument. However, AFM is very useful for the study of micro- and nanomorphological changes that may lead to the development of dendrites and other nonuniform phenomena, which seriously interfere with the possibility of using Li anodes in rechargeable batteries.

Figure 4 shows in situ CCD pictures of lithium electrodes in a PC/$LiAsF_6$ 0.5 M solution at OCV (4a), after cathodic charge transfer of about 0.08 C/cm^2 (4b) and after a Li deposition−

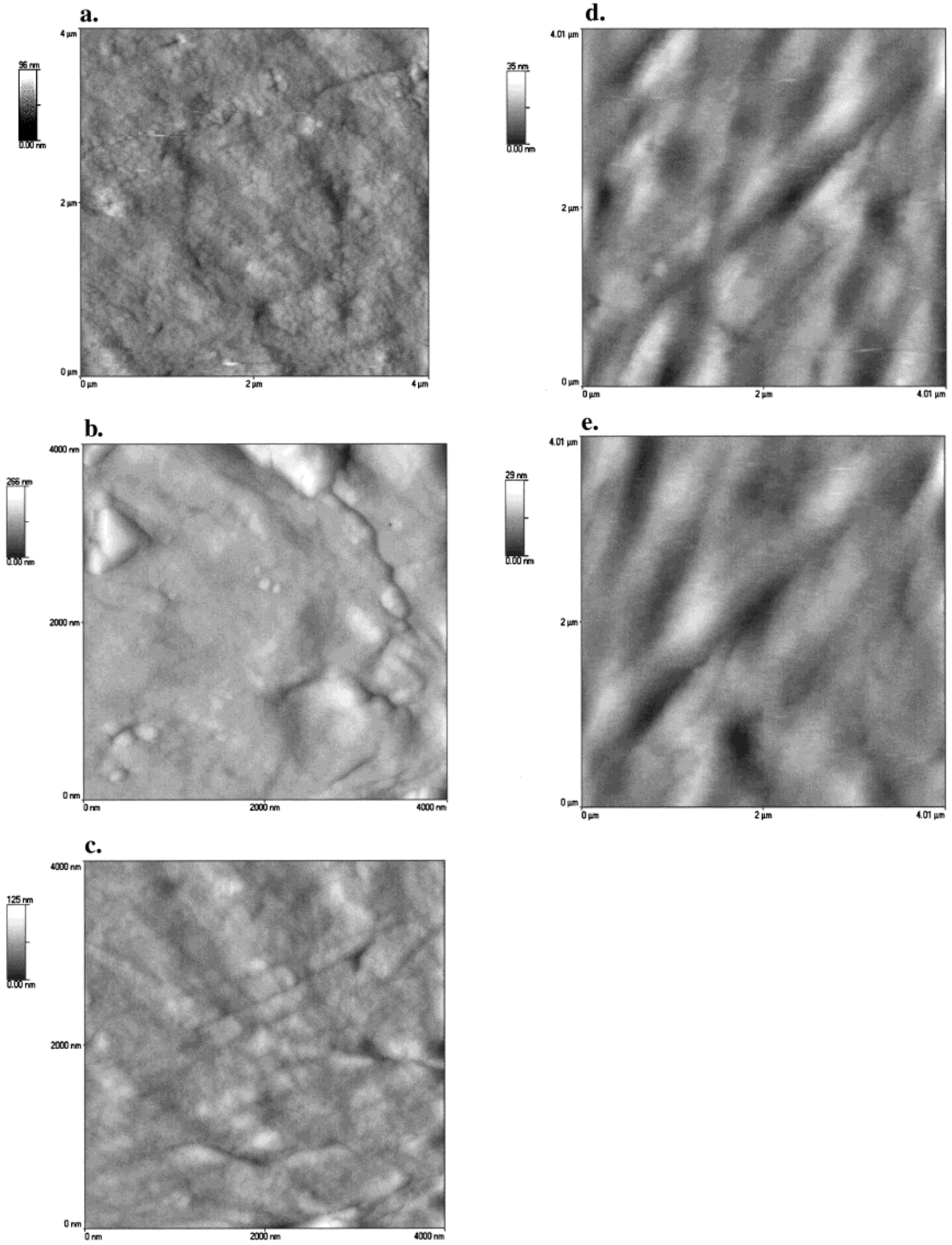

Figure 3. AFM images (4×4 μm) of Li electrodes aged in solution: (a) An image of the pristine electrode, Li under argon: (b) an AFM image of Li in EC-DEC 1:1 solution a few minutes after exposure; (c) same as b, after storage time of 50 min; (d) an AFM image of a Li electrode in a $LiAsF_6$/PC solution, a few minutes after immersion; (e) the same surface after 65 min of storage.

dissolution cycle (0.08 C/cm^2 for each process), followed by Li deposition (0.4 C/cm^2). Figure 5 shows the AFM images related to Figure 4, a and c (i.e., Li at OCV, and the electrode after several Li deposition−dissolution cycles). The processes related to Figures 4 and 5 were galvanostatic (0.8 mA/cm^2). From the pictures in Figure 4 and the images in Figure 5, it can be clearly seen that an important part of the charge transfer was involved in the formation of pronounced dendrites that were occasionally formed away from the AFM tip. The rest of the Li area underwent only minor morphological changes, as reflected in a comparison between the two images of Figure 5. It should be emphasized that the behavior shown in Figures 4 and 5 is not unique to PC/$LiAsF_6$ solutions and was, in fact, observed in all cases of Li electrodes in alkyl carbonate solutions, including experiments in which the current density was smaller, <0.4 mA/cm^2.

Figure 6a,b, related to EC-DMC solutions ($LiAsF_6$ and $LiPF_6$, respectively), presents AFM images of the same Li areas shown in the images of Figure 1b,c (respectively, measured at OCV) after two Li deposition−dissolution cycles, as indicated. Figure 6c,d shows images of Li electrodes in EC-DEC solutions ($LiAsF_6$ and $LiN(SO_2CF_3)_2$, respectively) after cycling (indi-

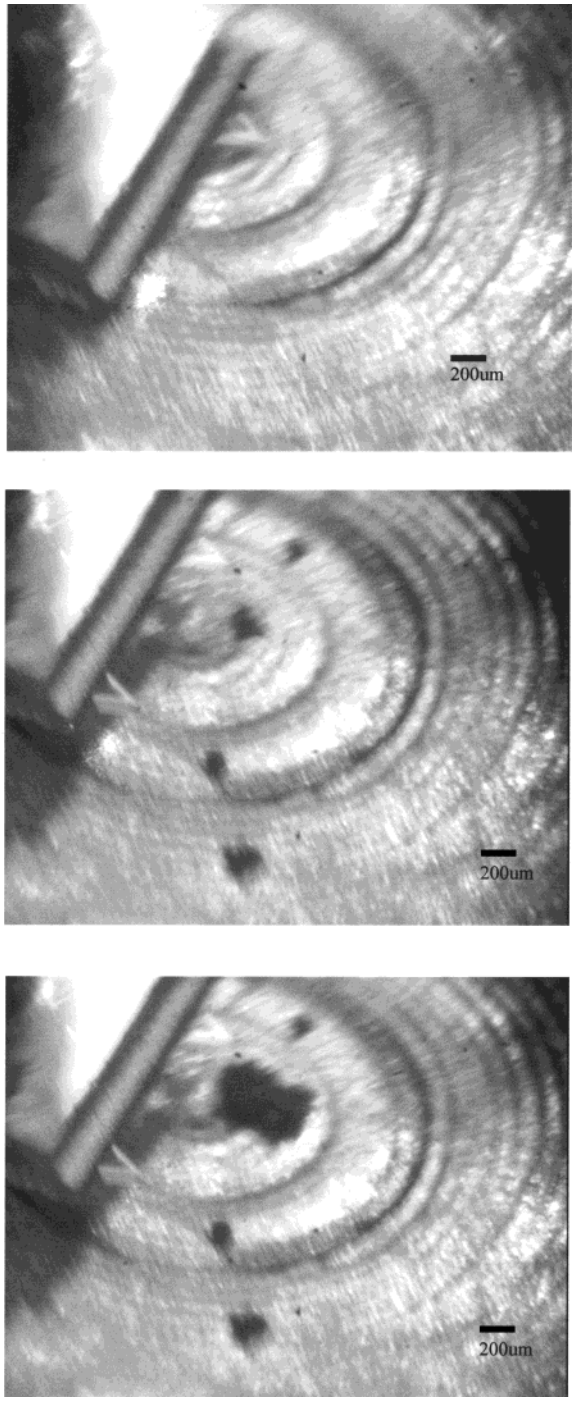

Figure 4. In situ CCD pictures of Li electrodes in $LiAsF_6$ 0.5 M/PC solutions. A scale appears in each picture. (a) The picture obtained at OCV. (b) The picture obtained after Li deposition, 0.08 C/cm^2. (c) The picture obtained after one Li deposition−dissolution cycle (0.08 C/cm^2), followed by Li deposition (0.4 C/cm^2). The current density in the various procedures was 0.8 mA/cm^2.

cated), that correspond to the images of the same Li areas (OCV) presented in Figure 1f,h, respectively. These images definitely represent the morphology of most of the Li area between dendrites. There are clear changes in the images, resulting from the electrochemical processes. However, all of them are in the nanometer scale. From these images it appears that in a great part of the electrode's surface there are processes that take place beneath the surface films that may lift them up as a result of Li deposition or push them down due to Li dissolution, without changing their basic morphology (cf. the relevant images in Figures1 and 6).

It is interesting to note that the presence of water in the alkyl carbonate solutions at centimolar concentrations (e.g., 200 ppm) may have a smoothing effect on the Li morphology, as demonstrated in Figure 7 (related to EC-DMC $LiAsF_6$ solutions as an example). We attribute this effect to the well-known secondary reaction of the surface species formed in alkyl carbonate solutions with water[19−20]

$$2ROCO_2Li + H_2O \rightleftharpoons Li_2CO_3 + CO_2 + 2ROH$$

We assume that substitution of the above organic Li salts (formed initially by the reduction of alkyl carbonates on the active metal)[19,20] by the inorganic carbonate (Li_2CO_3) forms more compact surface films, which are also smoother.

4. Dynamics of Li Deposition−Dissolution: Local Events That May Determine the Macromorphology of the Li Electrodes. We assume that the macromorphology of Li electrodes, which appear as dendrite formation, is determined by initial events that take place at centers of enhanced reactivity scattered on the lithium surfaces. These centers are probably points of pronounced nonuniformity of a nanometer scale, either in terms of chemical composition (and hence, electrical properties), or in terms of morphology (e.g., initial cracks, sharp edges, holes, etc.). In addition, we found that high current densities also lead to a pronounced nonuniformity of the surface films, which is clearly probed by AFM imaging. Of special interest is the effect of the high current density during Li dissolution. This is demonstrated in Figure 8, which shows images of a Li electrode treated in a $LiAsF_6$/PC solution at a current density of 0.8 mA/cm^2, which should be considered as a high current density for Li electrodes.[21] Images 8b and 8d, obtained after Li dissolution as the final process, are compared with images 8a and 8c, obtained after the preceding Li deposition processes.

It is clearly seen that the anodic processes (Li dissolution) at high current densities lead to cracks in the surface films. We explain these cracks as the result of the breakdown and repair of the surface films, which cannot accommodate the rapid changes in the morphology of the lithium layer underneath, as Li is depleted by fast electrochemical dissolution.

Figures9 and 10 demonstrate the situation of local nonuniformity of the Li surfaces, which are so typical of Li electrodes in all the alkyl carbonates/Li salt solutions studied herein. Image 9a shows two features (hills) formed during Li deposition in a $LiAsF_6$/PC solution (0.4 C/cm^2, 0.4 mA/cm^2). As shown in image 9b, consecutive Li dissolution in which the same amount of charge was involved, led to the disappearance of only one of the hills, while the neighboring feature remained untouched. We attribute this observation to a local nonuniformity in the electrochemical properties of the surface films. We assume that what we observe in the images of Figure 9 are Li deposition and dissolution beneath the surface films (i.e., no exposure of fresh lithium to the solution). While the anodic process is underway, the current density is intense at points at which the local ionic conductivity of the surface films is the highest. Hence, these results reflect nonuniformity of the surface films at the nanometer scale.

Images 10a−c show similar phenomena, as described above, occurring in EC-DMC/$LiC(SO_2CF_3)_3$ solution. Figure 10a relates to the electrode under open circuit in solution. Li deposition led to the formation of clear, well-distinguished Li deposits that appear as hills (see the marks in Figure 10b). It appears that most of these new features are formed near cracks and sharp edges initially present on the surface (due to the mechanical preparation of the electrode for the experiment). Hence, the initial geometry of the surface plays a role in directing the

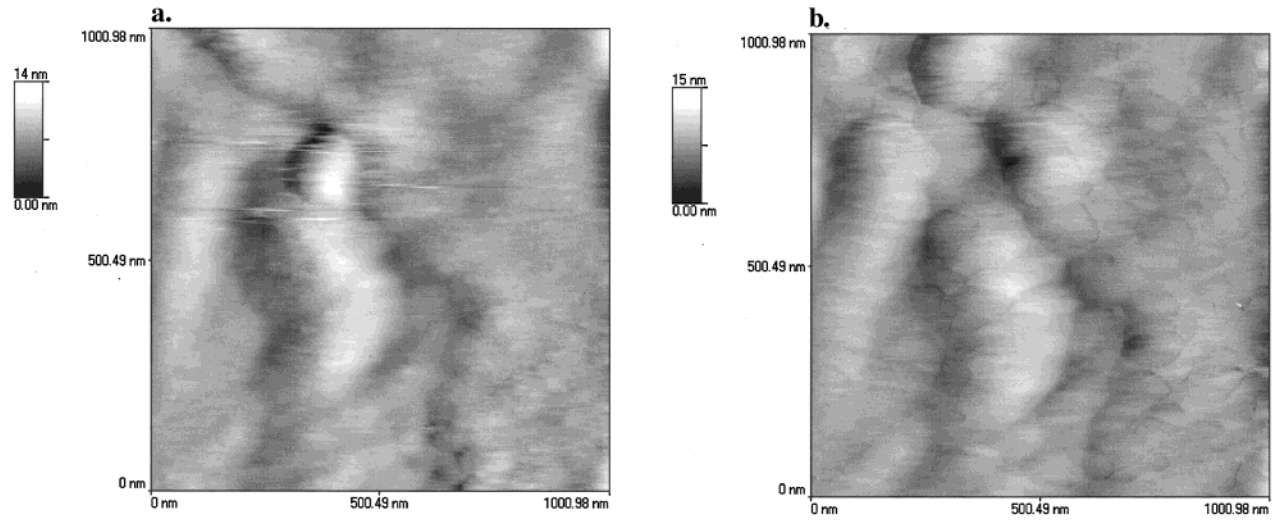

Figure 5. AFM images (1 × 1 μm) of the same electrode and solution as Figure 4, obtained during the same experiment: (a) an image measured at OCV; (b) an AFM image obtained after two Li deposition−dissolution cycles (0.08 and 0.04 C/cm^2), followed by Li deposition (0.8 C/cm^2).

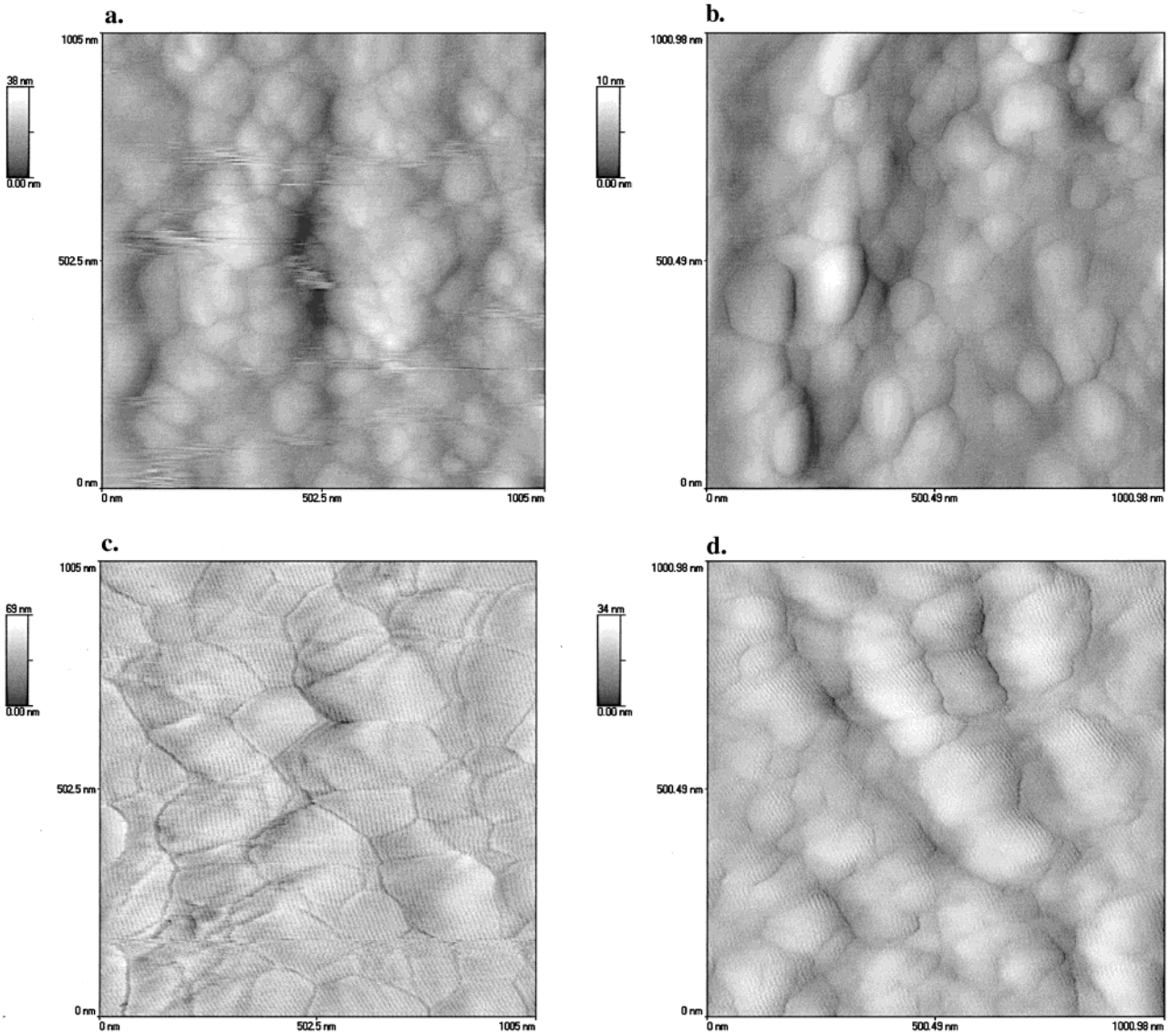

Figure 6. AFM images (1 × 1 μm) of a few of the Li surfaces, shown in Figure 1 at OCV, condition, after electrochemical processes (1 × 1 μm): (a) $LiAsF_6$ (0.5 M)/EC-DMC 1:1 solution, two Li deposition−dissolution cycles (0.08 and 0.4 C/cm^2 per process); (b) same as (a), 0.5 M $LiPF_6$ solution; (c) same as (a) and (b), $LiAsF_6$ (0.5 M)/EC-DEC 1:1 solution; (d) $LiN(SO_2CF_3)_2$ (0.5 M)/EC-DEC 1:1 solution, one Li deposition−dissolution cycle (0.08 C/cm^2 per process).

morphology of Li deposition due to the so-called primary current distribution, in addition to the influence of the secondary current distribution, resulting from the electrical properties of the surface films. Upon consecutive dissolution (see Figure 10c), only part

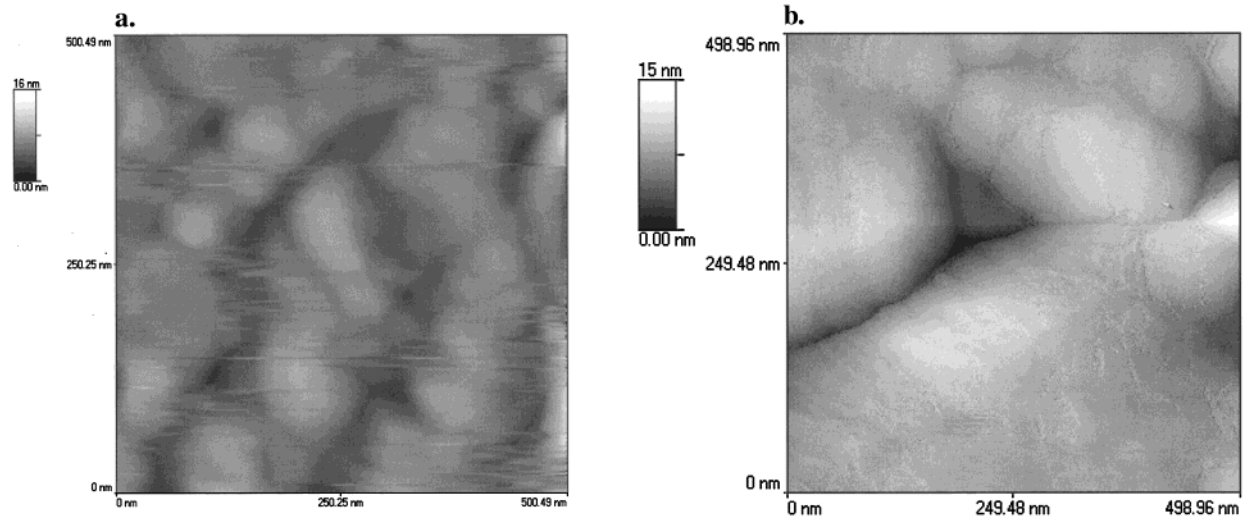

Figure 7. AFM images of Li electrodes after one Li deposition−dissolution cycle (0.08 C/cm^2) in $LiAsF_6$ 0.5/EC-DMC 1:1 solution (0.5 × 0.5 μm): (a) 20 ppm of H_2O; (b) 200 ppm of H_2O.

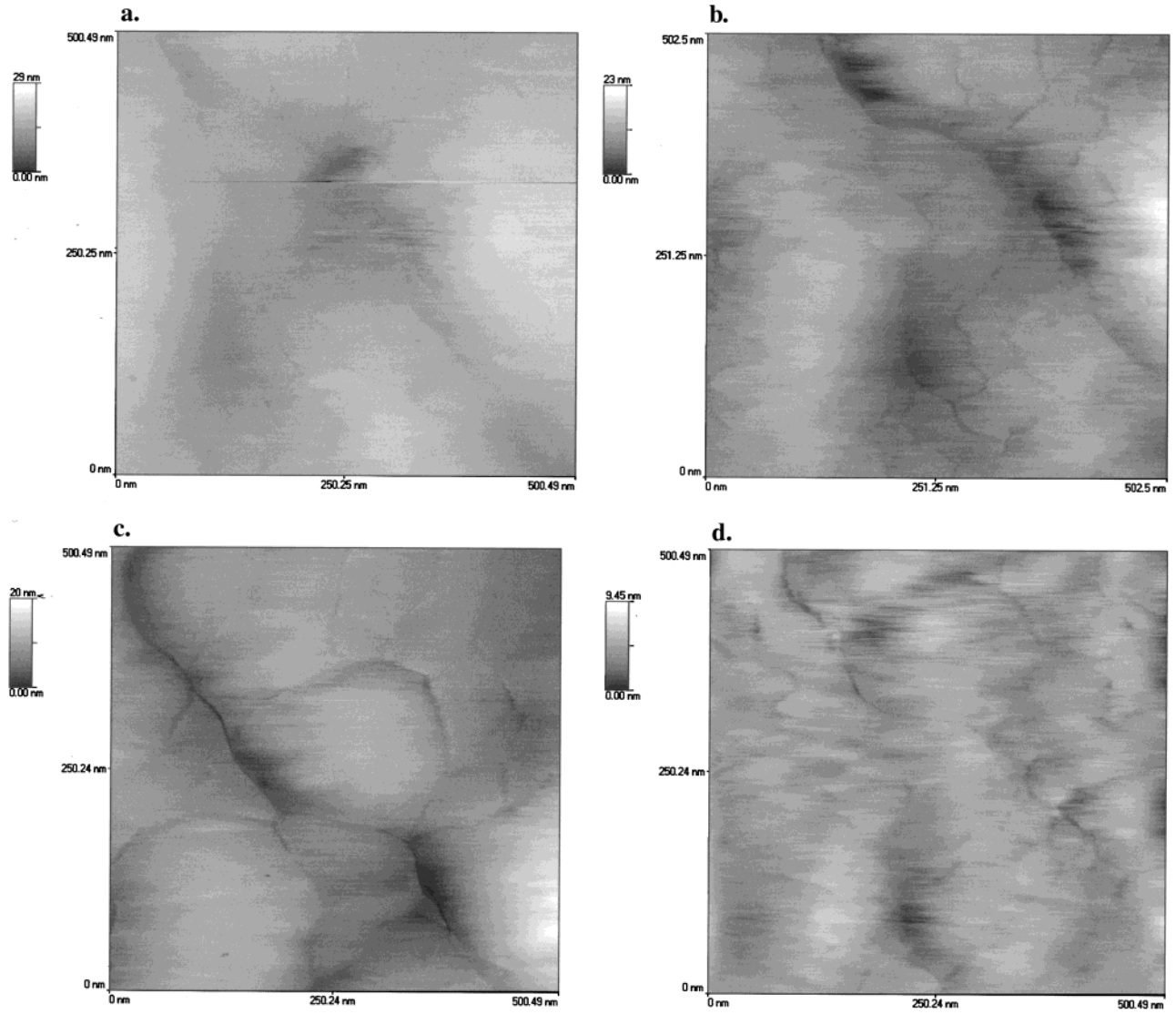

Figure 8. AFM images (0.5 × 0.5 μm) of Li electrodes processed at high current density: 0.82 mA/cm^2 in $LiAsF_6$ (0.5 M)/PC solution: (a) an AFM image of the Li electrode after Li deposition (0.08 C/cm^2); (b) same as (a), after consecutive Li dissolution (0.08 C/cm^2); (c) an AFM image of the Li electrode after two Li deposition−dissolution cycles (0.08 and 0.4 C/cm^2) followed by Li deposition (0.82 C/cm^2); (d) the same electrode as in (c), after three Li deposition−dissolution cycles (0.08, 0.4, and 0.82 C/cm^2).

of the Li deposits disappear (see the arrow marked in the image), while other features remained untouched. Hence, we again demonstrate the importance of the secondary current distribution (that we attribute to the local Li-ion conductivity of the surface

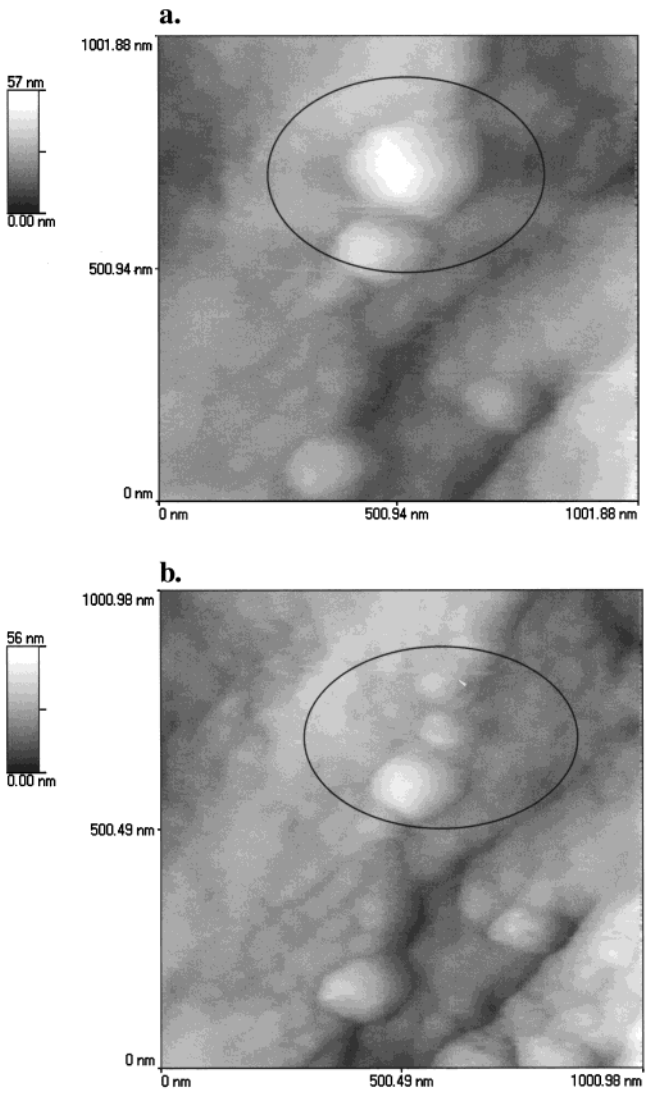

Figure 9. AFM images (1×1 μm) of a Li electrode in a $LiAsF_6$ (0.5 M)/PC solution. (a) An image obtained after Li deposition, 0.41 C/cm^2. New Li deposits are marked by a circle. (b) An image of the same area after consecutive Li dissolution (0.41 C/cm^2). The same area marked in (a) is also circled here.

films) in the determination of the nano- and micromorphology of the Li electrodes.

Summary and Conclusion

From previous intensive spectroscopic studies of Li electrodes,[19−25] it was concluded that the surface films which cover Li surface in the commonly used nonaqueous electrolyte solutions have a mosaic-type, multilayered structure, due to the large variety of possible surface reactions (as illustrated in Figure 2). The nanomorphological studies of Li electrodes by in situ AFM reflect the complicated structure of the surface films that cover this active metal in solutions. As clearly shown by previous spectroscopic studies,[20−25] unique surface reactions take place in each solution. These depend on the solvent, salt contaminants (H_2O, HF, Lewis acids), and the solubility of the possible reaction products in the solution. It should be noted that there are reactions of the electrophilic alkyl carbonate solvents with Li_2O and LiOH, which comprise the pristine (native) surface films, and direct reactions between lithium and solvent molecules which percolate through the pristine surface films. Therefore, in each solution both the surface chemistry

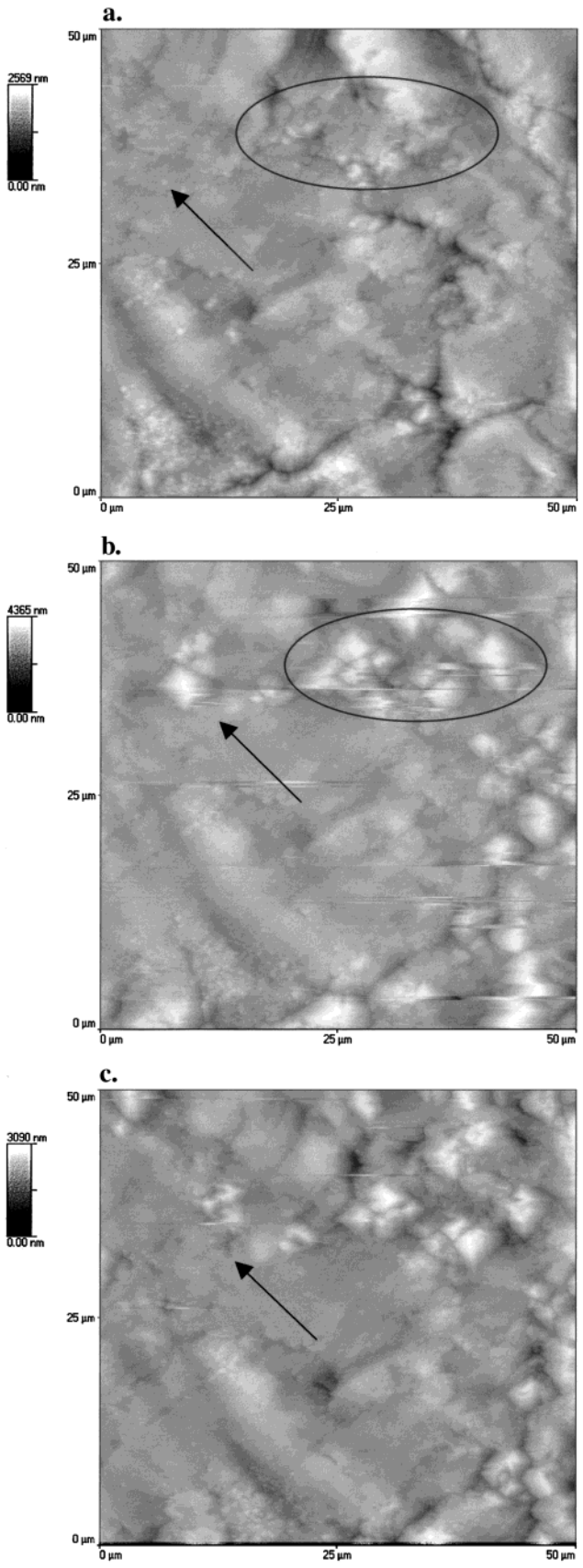

Figure 10. AFM images (50×50 μm) of a lithium electrode in a $LiC(SO_2CF_3)_3$ EC-DEC 1:1 solution: (a) The reference image of the electrode at OCV. (b) An image of the electrode after Li deposition (0.08 C/cm^2). The formation of new Li deposits are marked by a circle and an arrow. (c) An AFM image of the electrode after consecutive Li dissolution (0.08 C/cm^2). The arrow marks the location of a Li deposit that was dissolved (while the other deposits remained untouched).

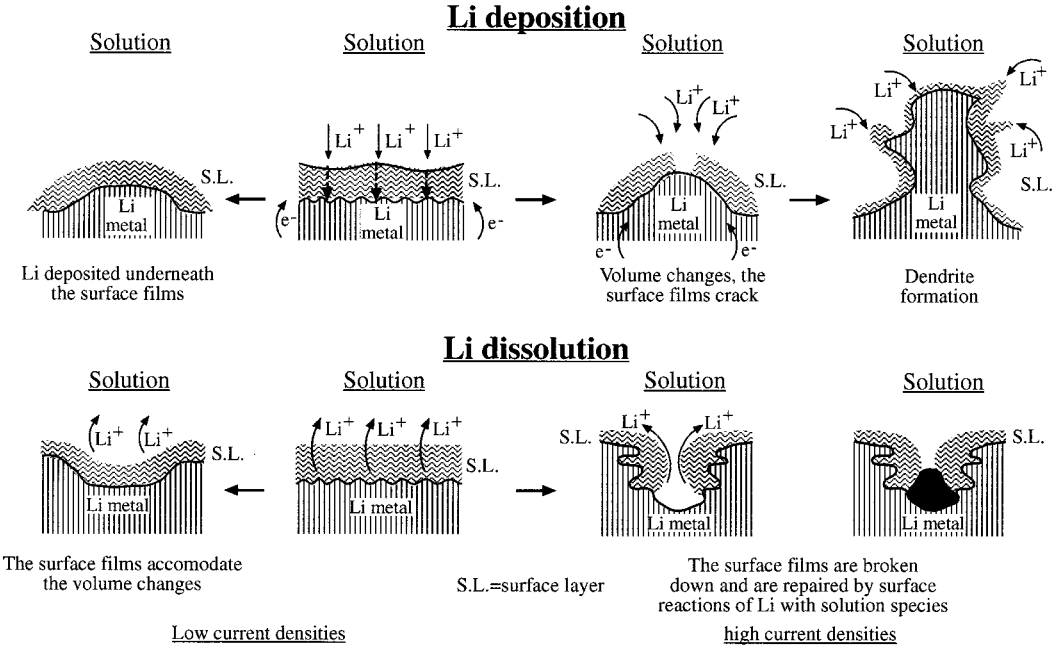

Figure 11. 11. An illustration of the morphological phenomena developed on Li electrodes during Li deposition and dissolution.

and the micromorphology differ. It seems that the nanomorphology of the Li surfaces in solutions at OCV clearly reflects the expected mosaic structure of the surface films, which are formed as a result of the complicated surface chemistry of the active metal in solutions. Hence, the surface films that cover the active metal are intrinsically nonuniform in the nanometer, and even in the micrometer, scale. It is generally accepted that the basic electrochemical behavior of Li electrodes is controlled by Li ion transport by migration through the surface films. Thus, the nonuniform chemical composition of the surface films means nonuniform, secondary current distribution when an electric field is applied, and Li deposition−dissolution takes place. Consequently, Li deposition is never uniform in any nonaqueous electrolyte solution. Initial rough morphology (e.g., sharp edges, cracks, etc.), spots of locally thin films, and nanometer size islands of surface species of high Li ion conductivity attract the electric current (i.e., the Li ion flux) and thus become points of intensive and preferred Li deposition.

Upon continuous Li deposition, part of the active metal is deposited beneath the surface films, as illustrated in Figure 11. In fact, most of the observations appearing in the images of Figures 5−10 reflect mild Li deposition beneath the surface films. However, in the case of alkyl carbonate solutions, the major surface species are Li salts such as $ROCO_2Li$, Li_2CO_3, LiF, etc., which cannot form highly cohesive surface films. Therefore, as the volume of the active metal changes due to a too-pronounced Li deposition, the protective surface films, composed of the above species, cannot accommodate the volume changes and thus crack, as illustrated in Figure 11. The cracks become the preferred locations for the electrochemical processes, and intensive Li deposition therefore occurs in these spots, thus leading to dendrite formation (as illustrated in Figure 11 and shown in Figure 4).

We found that there was a pronounced effect of the current densities applied on the Li electrodes' morphology during Li dissolution. At too high current densities, we see pronounced cracks on the surface films (Figure 8). As illustrated in Figure 11, we assume that the surface films cannot accommodate the morphological changes of the active metal, as Li is rapidly depleted beneath them. Hence, they are broken down and repaired by further reactions of the fresh lithium thus exposed, with solution species. On the basis of these observations and our understanding, we assume that a necessary condition for uniform, dendrite-free Li deposition, and hence, for the reversible behavior of Li anodes, is the formation of flexible surface films that can better accommodate the morphological changes of the Li electrodes during Li deposition or Li depletion than the surface films formed on lithium in the alkyl carbonate solutions studied herein. As recently discussed, flexible surface films may be found on lithium in some cyclic ethers (e.g., 1−3 dioxolane) and in polymer electrolyte based on poly(ethylene oxide) (PEO) and its derivatives.[26]

Acknowledgment. Partial support for this work was obtained from the New Energy Development Organization (NEDO) Japan, and from the German Ministry of Science (BMBF), within the framework of the DIP Program for Israeli-German collaboration.

References and Notes

(1) Dominey, L. in *Nonaqueous Electrochemistry*; Aurbach, D., Ed.; Marcel Dekker: New York 1999; Chapter 8, p 437.

(2) Fugieda, T.; Yamamoto, N.; Saito, K.; Ishibashi, T.; Hanjo, M.; Koike, S.; Wakabayashi, N.; Higuchi, S. *J. Power Sources* **1994**, *22*, 99.

(3) Aurbach, D. *J. Electrochem. Soc.* **1989**, *136*, 1610.

(4) Radman, D. The Electrochemical Society Fall Meeting, New Orleans, October 1984. *Extended Abstracts*; The Electrochemical Society Inc.: Pennington, NJ, 1984; PV 84−2, p 188.

(5) Aurbach, D.; Weissman, I. *Electrochem. Commun.* **1999**, *1*, 324.

(6) Peled, E. In *Li Batteries*; Gabano, J. P., Ed.; Academic Press: London, 1983; Chapter 3, p 43.

(7) Osaka, T.; Momma, T.; Nishimura, K.; Tajima, T. *J. Electrochem. Soc.* **1993**, *140*, 2745.

(8) Kanamura, K.; Shiraishi, S.; Takehara, Z. I. *J. Electrochem. Soc.* **1996**, *143*, 2187.

(9) Lafage, M.; Windel, D.; Russier, V.; Badiali, J. P. *Electrochim. Acta* **1997**, *42*, 2841.

(10) Fringarnt, C.; Tranchant, A.; Messina, R. *Electrochim. Acta* **1995**, *40*, 513.

(11) Aurbach, D.; Zinigrad, E.; Teller, H.; Dan, P. *J. Electrochem. Soc.* **2000**, *147*, 1274.

(12) Armand, M. The International Meeting on Li Batteries, "Li 2000", Como, Italy, May 28−June 2, 2000. *Extended Abstract*; The Electrochemical Society Inc.: Pennington, NJ, 2000; Abstract 26.

(13) Naoi, K.; Mori, M.; Inone, M.; Wakabayashi, T.; Yamauchi, K. *J. Electrochem. Soc.* **2000**, *147*, 803.

(14) Wang, X.; Yasukawa, E.; Mori, S. *J. Electrochem. Soc.* **1999**, *146*, 3993.
(15) Aurbach, D.; Cohen, Y. *Rev. Sci. Instrum.* **1999**, *70*, 4668.
(16) Aurbach, D.; Cohen, Y. *J. Electrochem. Soc.* **1996**, *143*, 3525.
(17) Aurbach, D.; Cohen, Y. *J. Electrochem. Soc.* **1997**, *144*, 3355.
(18) Aurbach, D.; Cohen, Y. *Electrochem. Solid State Lett.* **1999**, *2*, 16.
(19) Aurbach, D.; Daroux, M. L.; Faguy, P.; Yeager, E. B. *J. Electrochem. Soc.* **1887**, *134*, 1611.
(20) Aurbach, D.; Gofer, Y.; Ben-Zion, M.; Aped, P. *J. Electroanal. Chem.* **1992**, *339*, 451.
(21) Aurbach, D.; Weissman, I.; Yamin, H.; Elster, E. *J. Electrochem. Soc.* **1998**, *145*, 1421.
(22) Goren, E.; Chusid, O.; Aurbach, D. *J. Electrochem. Soc.* **1991**, *138*, L6.
(23) Aurbach, D.; Ein-Eli, Y.;. Zaban, A *J. Electrochem. Soc.* **1994**, *141*, L1.
(24) Kanamura, K.; Tamura, H.; Shiraishi, S.; Takehara, Z. I. *J. Electroanal. Chem.* **1995**, *394*, 49 and references therein.
(25) Schechter, A.; Aurbach, D. *Langmuir* **1999**, *15*, 3334.
(26) Aurbach, D. *J. Power Sources* **2000**, *89*, 206.